



**South-West University "Neofit Rilski"
Faculty of Mathematics and Natural Sciences
Department of Chemistry**

MARIO YORDANOV MITOV

**ELECTROCHEMICAL SYSTEMS
FOR GREEN ENERGY PRODUCTION**

AUTOREFERAT

**OF DISSERTATION
TO AWARD A DEGREE**

DOCTOR OF SCIENCES

**in scientific field 4. Natural Sciences, Mathematics and
Informatics**

scientific direction 4.2. Chemical Sciences

Specialty "Inorganic Chemistry"

BLAGOEVGRAD

2019

The dissertation is written on 296 pages, A4 format (without apps). It contains 186 figures, 36 tables, and 5 schemes. 319 literary sources are cited. The dissertation is structured in the following sections: Introduction; Purpose and tasks; Alternative chemical fuel cells presented in 2 subsections; Bioelectrochemical systems for electricity generation and hydrogen production presented in 9 subsections; Conclusions; Contributions; References; Supplement; List of publications included in the dissertation.

Note: The original numbering of the figures, tables, schemes, and citations of the dissertation is preserved in the autoreferate, while the sections and subsections are renumbered.

Author: Mario Yordanov Mitov

Title: **Electrochemical systems for green energy production**

INTRODUCTION

Against the backdrop of exhausting natural fuels and a progressively growing population, one of the greatest challenges in the early 21st century is to solve the problem of ever-increasing energy consumption. In turn, the use of traditional carbon-containing fuels to meet energy needs leads to a dangerously increasing pollution of the environment. In this respect, the use of new, more environmentally friendly sources and energy converters is becoming one of the most crucial and urgent tasks of our time.

The greatest hope in this direction is assigned to the concept of the hydrogen economy. At the heart of this concept is the idea of hydrogen, produced from renewable sources, to be delivered to end users, where its chemical energy is transformed into electricity using fuel cells.

To avoid the inconvenience of existing storage methods and the lack of built infrastructure for hydrogen transportation, there has been strong research interest in the development of alternative hydrogen fuel cell technologies over recent decades. Some of the studies are aimed at exploring the possibilities of using hydrogen-rich solid or liquid compounds. Of particular interest in this aspect are the alkali borohydrides. In addition to the high hydrogen content (7.4 to 18.3 wt.%), the electrochemical oxidation of borohydrides is carried out with the participation of a large number of electrons, making them a convenient and safe solution for the storage and transport of hydrogen as well as for direct use in fuel cells. Another interesting alternative is the oxidation of sulfides, which along with the generation of electricity would have an ecological effect for their purification.

One of the newest varieties of classic fuel cells is biofuel cells, better known as microbial fuel cells (MFCs). Using living microorganisms as biocatalysts, MFCs are able to convert the

chemical energy of waste products into useful substances and electricity. Under certain conditions, MFC biocatalysts can be used in so-called microbial electrolyzers, which significantly reduce the energy for electrolysis of water. Microbial electrolysis technology has been intensively developed only in the last 5 years but has now become a new prospect for hydrogen generation.

This dissertation thesis covers major achievements in the development of new types of fuel cells and electrolyzers, which are part of the most modern trends in the development of alternative energy converters over the last 15 years.

PURPOSE AND TASKS

The purpose of this dissertation thesis is to systematize the main results and achievements of the implementation of a long-term research program aiming at the creation of innovative (bio) electrochemical systems for electricity and hydrogen generation.

During the implementation of the program, the following main **tasks** have been set and implemented:

1. Synthesis and testing of new electrocatalysts as potential electrode materials for (bio)fuel cells and microbial electrolysis cells.

2. Design and complex testing of different types of (bio) electrochemical systems for generating electric current and hydrogen, including:

- fuel cells with direct electrooxidation of borohydride;
- fuel cells with sulfide electrooxidation;
- microbial fuel cells using pure and mixed cultures as biocatalysts;
- microbial electrolysis cells.

3. Investigation of the mechanism of the processes in the realized (bio)electrochemical systems.

4. Possible applications of created (bio)electrochemical systems.

I. ALTERNATIVE CHEMICAL FUEL CELLS

I.1. Direct borohydride fuel cells (DBFC)

The main problem in the development of DBFC is that most of the materials exhibiting high electrocatalytic activity with respect to the anodic oxidation of borohydrides are also good catalysts for their hydrolysis - a reaction leading to unproductive decomposition and reduction of the efficiency of its utilization as fuel. One of the main objectives of our DBFC research is to find such hydrogen-adsorbing anode materials and conditions where the degree of hydrolysis of the borohydride is minimal.

1.1.1. Examination of hydrogen-absorbing alloys and composites as potential anode catalysts for borohydride electrooxidation

A complex methodology has been developed to study the electrocatalytic properties of electrode materials in relation to the direct electrooxidation reaction of borohydride and to evaluate the proportion of possible parallel reactions - hydrolysis and absorption of hydrogen in the electrode material, by which the effect of this decomposition is reduced and "secondary storage" of the fuel is accomplished.

Metal hydride alloys and hydrogen-absorbing nanocomposites are investigated as potential anode materials for DBFCs, which according to their chemical composition and method of preparation can be classified into the following three groups:

- Metal hydride alloys of AB₅ type, conventionally used in Ni-MH batteries;
- Cobalt-based ternary and quaternary nanocomposites, not containing precious metals;
- Pd-Au composites deposited on Ni-foam.

1.1.1.1. Behavior of AB_5 metal hydride electrodes in a borohydride-containing electrolyte

It has been found that when treating the electrodes with $NaBH_4$ solution, an identical hydride phase is formed in the alloys as well as after an electrochemical charge when operating in a Ni-MH battery.

The results obtained show that the sorption capacity of the electrodes treated in borohydride solution is close to that of the initial charge/discharge cycles of MH electrodes operating in alkaline Ni-MH batteries - Fig. 9.

Higher values, close to the nominal discharge capacity of the "activated" metal hydride electrode (~ 320 mAh/g), are achieved with electrodes made from a powdered alloy pretreated in a borohydride solution, which is assigned to the transformation of the entire amount starting alloy in tertiary metal hydride (β -phase). The method may find application to simplify the process scheme for the manufacture of Ni-MH rechargeable batteries.

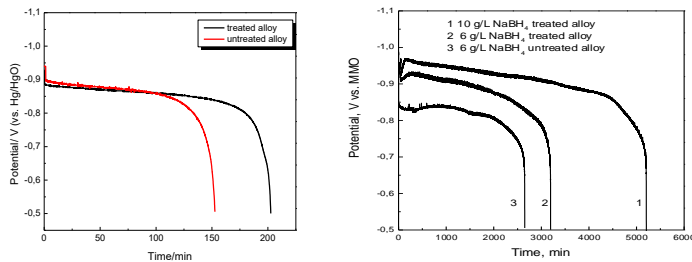


Fig. 9. Discharge curves obtained with MH electrodes made from AKL-86 alloy in 6M KOH electrolyte after 12 hours of treatment in 2 g/l $NaBH_4$, $j_{disch.} = 10$ mA.cm⁻². (left)

Fig.11. Discharge curves obtained with MH electrodes in alkaline electrolytes with different concentrations of $NaBH_4$; $j_{disch.} = 10$ mA.cm⁻². (right)

The investigated electrodes show a significantly higher discharge capacity in alkali electrolytes of NaBH₄ due to the direct electrooxidation of borohydride (Figure 11). The discharge capacity values vary depending on the particular composition of the electrode material, the borohydride concentration and the operating temperature. The largest discharge capacity is achieved with electrodes from the AKL-86 alloy in 5% NaBH₄/ 6M KOH electrolyte. With increasing operating temperatures, the discharge capacity increases from 1300 mAh at room temperature to 1800 mAh at 60 °C, resulting in an increase in coulombic efficiency (the usability of sodium borohydride as a fuel) from 5.3 to 21.2 %. The obtained coulombic efficiency values are comparable to those (19-23%) reported by other authors using metal hydride AB₅ alloys as anodes in DBFC [48].

It has been experimentally proven that the main reason for the difference in the behavior of the alloys studied under identical conditions is their different catalytic activity against the "non-productive" degradation of the borohydride by hydrolysis. The highest catalytic activity with respect to the hydrolysis of sodium borohydride has the AKL-1519 alloy, and the lowest AKL-86 (Table 3), which supports the hypothesis that the greater discharge capacity using AKL-86 electrodes is due to the slower depletion of the borohydride as a result of its hydrolysis.

Table 3. Hydrogen generation rate [ml/s] of sodium borohydride at 25 °C.

Electrode material	AKL-86	AKL-1002	AKL-1519
V(H ₂) [ml/s]	5,0.10 ⁻⁴	11,4. 10 ⁻⁴	60,3. 10 ⁻⁴

It has been found that at the same concentration of NaBH₄ in the electrolyte the rate of hydrolysis of the borohydride decreases with the increase in the current density due to the competition

between the two processes - electrooxidation and hydrolysis of the borohydride, and it is obvious that with greater efficiency the fuel would be utilized in a fuel cell with direct oxidation of borohydride at higher current loads. The resulting kinetic dependencies (Figure 15) are linear, which indicates the zero order of the hydrolysis process.

Based on the calculated relative share of the three reactions - borohydride electrooxidation, hydrolysis and hydrogen absorption over the analytically determined depletion of the sodium borohydride in the electrolyte, the best correspondence of the obtained results and the hypothesis for the participation of 2 electrons in the electrooxidation process has been found.

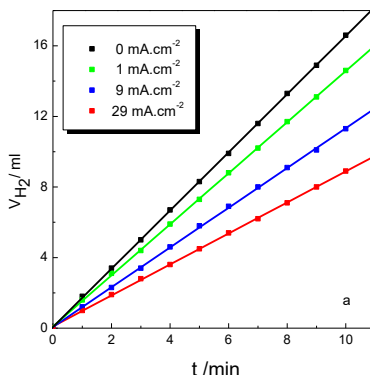


Fig.15. Kinetic curves for hydrogen evolution on MH-electrodes in 5% NaBH₄ / 6M KOH electrolyte at different current densities.

1.1.1.2. Catalytic activity of hydrogen-absorbing nanocomposites with respect to the electrooxidation and hydrolysis of sodium borohydride

The behavior of electrodeposited on Ni-foam ternary and quaternary nanocomposites (CoMnB, CoNiMnB, CoNiMoW) in alkaline solutions of sodium borohydride is investigated. The

hydrogen-absorbing properties of these materials are determined by characteristic potentials for the electrochemical hydrogen desorption (ca. -0.8V vs. Hg/HgO) of the formed plateau in the discharge curves obtained in an alkaline electrolyte (Figure 26).

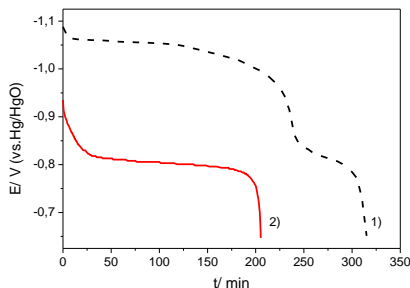


Fig.26. Discharge curves obtained with CoMnB electrode in: 1) $0.1\text{M NaBH}_4/6\text{M KOH}$; $I_{\text{disch}} = 5\text{mA}$; 2) 6M KOH (after treatment in NaBH_4 solution); $I_{\text{disch}} = 2\text{mA}$.

At low discharge currents, two well-defined plateaus are observed on the discharge curves obtained in the borohydride-containing electrolyte. The first, longer plateau is formed at potentials more negative than -1.0V (vs. Hg/HgO) and corresponds to the borohydride electrooxidation, while the second, shorter plateau occurs at MH-electrode specific potentials. Taking into account the different discharge currents applied, it is calculated that the discharge capacity corresponding to the second plateau in curve 1) is almost the same as that calculated by curve 2). The second plateau corresponds to the electrooxidation of hydrogen absorbed in the electrode material and demonstrates the capabilities of this type of electrodes for storage and subsequent use of hydrogen as a "secondary" fuel.

The presence of Ni in electrodepositions increases electrocatalytic activity with respect to borohydride oxidation. However, the achieved discharge capacity values for $\text{CoNiMnB}/$

Ni-foam electrodes (~ 400 mAh/g NaBH₄) are lower than those for the MH-electrodes tested (~ 900 mAh/g NaBH₄ for AKL-86).

Differences in composition and conditions of preparation also lead to the different catalytic activity of the investigated nanocomposites with respect to the hydrolysis of borohydride (Table 5).

Table 5. Hydrogen generation rate and activation energy of the sodium borohydride hydrolysis process catalyzed by the investigated Co-containing nanocomposites [55].

Material	Hydrogen generation rate (ml/s)				E _a (kJ/mol)
	16°C	25°C	30°C	40°C	
CoMnB	0.061	0.162	0.277	0.501	54.9
CoNiMnB	0.901	1.300	1.402	2.101	36.9
CoNiMoW	0.063	0.076	0.115	0.252	37.8

The combination of a relatively long discharge time without refueling, small overpotentials at high discharge current densities and a relatively high rate of hydrogen evolution resulting from borohydride hydrolysis is suitable for use of the developed CoNiMnB catalysts in hybrid DBFC/HOD systems. Due to its high purity and humidity, the hydrogen generated during the operation of the direct borohydride fuel cell could directly feed another low-temperature hydrogen fuel cell (PEMFC or AFC). Moreover, the rate of the two competing processes - electro-oxidation and hydrolysis of the borohydride can be regulated by the applied discharge current density (Figure 31).

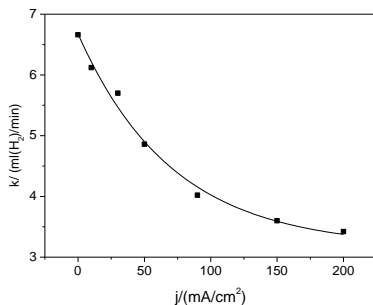


Fig. 31. Dependence of hydrogen evolution rate on CoNiMnB electrode in the borohydride-containing alkaline electrolyte on current density.

Because of the lowest hydrolysis rate recorded compared to the other cobalt-based catalysts, CoNiMoW/Ni-foam electrodes are directly tested as DBFC anodes.

1.1.1.3. Electrocatalytic activity of bimetallic Pd-Au catalysts in alkaline solutions of sodium borohydride

Along with non-precious metal catalysts, a series of bimetallic Pd-Au catalysts has been synthesized and tested as potential anodes for DBFC. The maximum power values obtained with the three Pd-Au catalysts exceed with an order of magnitude that obtained with the unmodified nickel foam (Figure 35), which reveals their potential as anodic catalysts for DBFC.

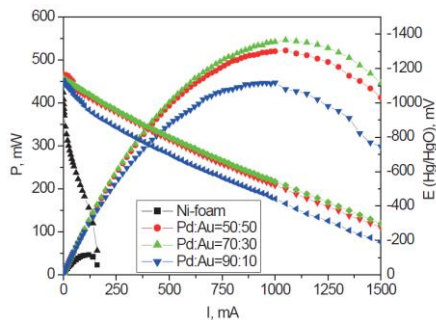


Fig. 35. Polarization curves and power curves obtained with Pd-Au/ Ni-foam and nickel foam without catalyst in 5% NaBH₄ / 6M KOH electrolyte.

Similar to the AKL series MH-alloys tested, the pretreatment of the samples in sodium borohydride solution increased almost double the power achieved (Table 7). The observed activation is assigned to the hydrogen-absorbing ability and the formation of a stable metal hydride with Pd, which is subsequently involved in the current-generation reaction.

Table 7. Operation characteristics achieved with the Pd-Au catalysts tested.

Catalyst	Untreated catalyst		Catalyst treated in 1.3 M NaBH ₄ / 6M KOH		Discharge capacity Q, mAh
	I, mA	P, mW	I, mA	P, mW	
Pd:Au=50:50	460	224	1050	522	900
Pd:Au=70:30	640	332	1100	543	975
Pd:Au=90:10	640	263	960	447	1100

The highest discharge capacity (1100 mAh or 730 mAh g⁻¹ NaBH₄) at constant current load is achieved with Pd-Au (90:10)/ Ni-foam regardless of the lower current and power values

achieved by the polarization curves. This result is most likely due to the higher Pd content in the deposit, providing greater sorption capacity in terms of hydrogen storage, which in turn acts as an additional "secondary" fuel in the anode oxidation process.

1.1.2. Construction and testing of DBFC with selected anodes and air cathodes

Based on the lowest hydrolysis rates determined by the catalytic experiments in sodium borohydride solution, electrodes made from the AKL metal hydride alloys and CoNiMoW nanocomposites are tested as anodes in DBFC. Typical polarization curves and power curves taken with the three types of AKL anodes in a monolithic cell with one air cathode are shown in Fig. 38.

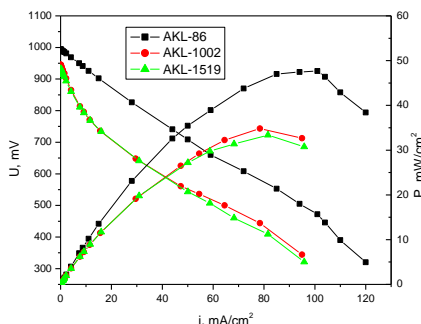


Fig. 38. Polarization curves and power curves of a fuel cell with AKL-86, AKL-1002, AKL-1519-anodes in 5% NaBH₄ / 6M KOH.

As with tests in the three-electrode cell, the highest electrical characteristics (generated current and power) are achieved with AKL-86 electrodes.

In order to establish the effect of the direct contact between the cathode and the borohydride-containing electrolyte, a series of experiments are carried out, in which a proton exchange

membrane Nafion[®] 117 (DuPont) is assembled on the surface of the gas-diffusion cathode. The results of the polarization measurements show that the membrane increases the internal resistance of the cell and reduces its power (Figure 39). On the other hand, the use of a membrane increases the discharge time, resp. the efficiency of using sodium borohydride as a fuel (Figure 40).

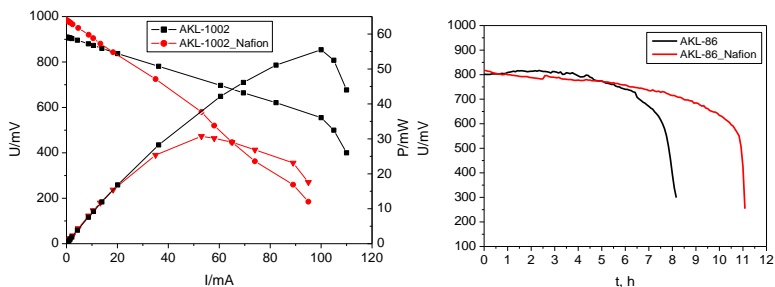


Fig. 39. Polarization curves and power curves of a fuel cell with AKL-1002 anode and air cathode in 5% NaBH₄/6M KOH with and without Nafion membrane (left)

Fig. 40. Discharge curves of fuel cell with AKL-86 anode and air cathode in 5% NaBH₄/6M KOH with and without Nafion membrane (right)

The most likely explanation for increasing the discharge capacity of membrane-electrode assembly is that the contact between the electrolyte and the cathode is prevented, which reduces the "non-productive" degradation of the sodium borohydride due to catalyzed hydrolysis or chemical oxidation by the oxygen.

Significant improvement in performance has been achieved with the use of a fuel cell with two air cathodes. Despite the close DBFC performance achieved in the variable load polarization

experiments, the calculated discharge capacity of 300 mAh g⁻¹ NaBH₄ using CoNiMoW is 2.3 times less than that achieved with the AKL-86 anode (700 mAh g⁻¹ NaBH₄) and quite below the theoretical capacity of the borohydride (5.67 Ah g⁻¹ NaBH₄). The main reason for the lower efficiency of the fuel utilization for DBFC with CoNiMoW anodes is the catalytic activity of the nanocomposite catalysts with respect to the non-productive degradation of the borohydride by hydrolysis. Although the lowest of the Co-containing nanocomposites tested, the rate of borohydride hydrolysis on CoNiMoW is several times higher than that of MH-alloys even at high current loads.

The obtained results suggest that DBFCs with an anode of hydrogen-absorbing materials and air cathodes are suitable as emergency uninterruptible power supplies (UPS) that can operate continuously at low current loads (up to 50 mA) for 5 to 10 hours without recharging of the fuel. The MH-alloy AKL-86 is the most suitable of the anode materials studied so far. The resulting current and power density values using the AKL-86 anode and air cathode are comparable to those reported in the literature for similar systems [37].

I.2. Fuel cells with sulfide electrooxidation

I.2.1. Electrooxidation of sulfides in a fuel cell with various cathodic oxidants

The principle of operation of a fuel cell with sulfide electrooxidation has been confirmed experimentally by the use of a double-chamber cell and various oxidants dissolved in the catholyte as final electron acceptors. It is found that regardless of the composition of the catholyte used, the operating characteristics of the fuel cell increase with increasing the concentration of sulfide (Figure 49) and the pH of the anolyte (Figure 50). The highest values of the generated current and maximum power are achieved with a FeCl_3 cathodic oxidant.

Multiple increases in the values of the generated current and maximum power are achieved by replacing the graphite electrodes with carbon felt and the use of a proton-exchange membrane (Nafion[®] 117) - Fig. 51.

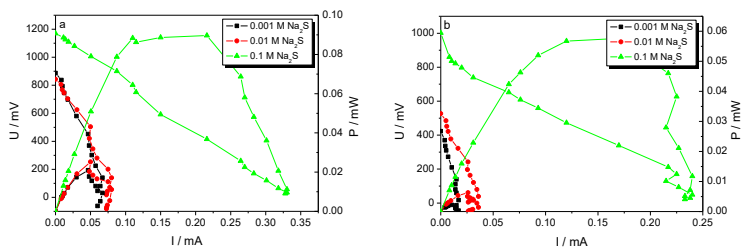


Fig. 49. Polarization curves and power curves obtained with anolytes with different concentrations of Na_2S and catholyte: a) FeCl_3 ; б) $\text{K}_2\text{Cr}_2\text{O}_7$.

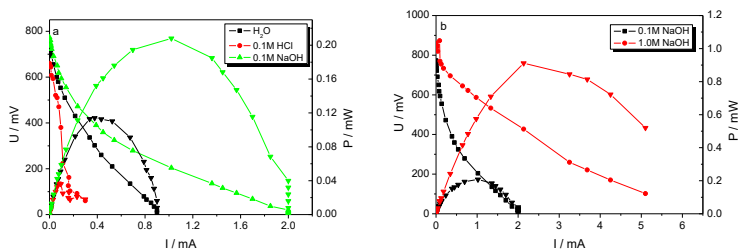


Fig. 50. Polarization curves and power curves of a sulfide fuel cell with graphite electrodes at different pH of the anolyte.

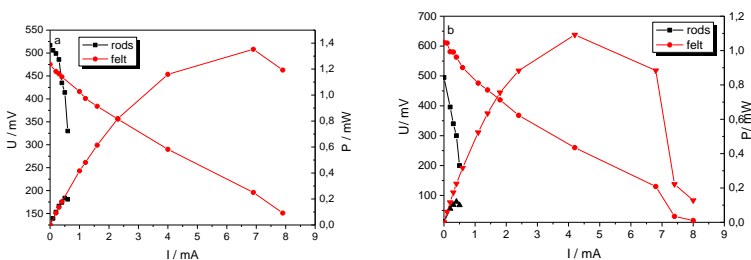


Fig. 51. Polarization curves and power curves obtained with different carbon electrodes (graphite rods and carbon felt), anolyte 0.1 M Na_2S and catholyte: a) FeCl_3 ; b) $\text{K}_2\text{Cr}_2\text{O}_7$.

The development of a fuel cell in which the electrooxidation of sulfides on the anode and the electroreduction of nitrates on the cathode takes place is a promising possibility for simultaneous desulfidation and denitrification of waters containing these pollutants. With the use of H-type fuel cell with Nafion[®] 117 membranes, a five-fold increase in current values compared to those obtained from a salt bridge fuel cell operating under identical conditions (Figure 53) has been achieved. The registered significant decrease in current after the 10th hour is associated with the depletion of sulfides in the anolyte, confirmed by the quantitative analysis.

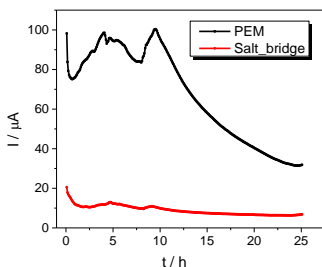


Fig. 53. Variation in current at the operation of a fuel cell with PEM and a salt bridge with concentrations of 50 mg/l sulfides and nitrates, respectively in anolyte and catholyte; $R_{ext.} = 100\Omega$.

Within 25 hours, sulfides are completely depleted in the fuel cell with PEM, leading to a significant reduction in generated current. The current generation at the end of the experiment is most likely due to the formation of sulfur intermediates, which undergo further oxidation on the anode.

Parallel to the study of the anodic semi-reaction, the concentration of nitrates and nitrites in the catholyte is also analyzed. It has been found that during the process a minimum amount of nitrates is reduced to nitrite, which gives reason to conclude that in the abiotic sulfide-nitrate fuel cell the cathodic reaction is mainly associated with the reduction of oxygen.

1.2.2. Electrodeposited NiW and NiMoW catalysts for sulfide oxidation

Applying the additive principle proposed by Wagner and Traud [96], the kinetics of sulfide oxidation on NiW and NiMoW catalysts, obtained by electrodeposition on nickel mesh and nickel foam, is studied. By recording the partial cathode and anode polarization curves (Figure 60), respectively in an aerated solution of NaOH and alkaline solution of Na₂S under anaerobic

conditions, the values of the mixed potential E_{mix} and the mixed current I_{mix} are determined.

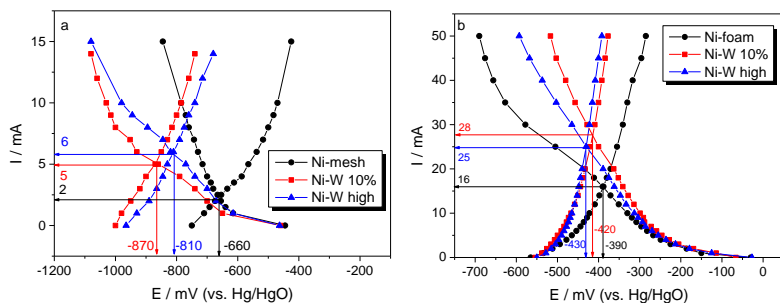


Fig. 60. Polarization curves obtained with: a) NiW/Ni-mesh and Ni-mesh; b) NiW/Ni-foam and Ni-foam: catholyte - 0.25M NaOH; anolyte- 0.4M Na₂S + 0.25M NaOH, continuously purged with nitrogen.

The steeper anodic curves corresponding to a lower anode polarization are indicative that the kinetics of the sulfide oxidation on the catalysts explored is limited by the oxygen reduction half-reaction. On the other hand, the close values of the measured open circuit potential (OCP) in the presence of sulfide ions and oxygen and of the mixed potential E_{mix} determined by the polarization curves are an indication that the process is carried out by an electrochemical mechanism. The higher catalytic activity of deposited NiW nanocomposites compared to unmodified nickel electrodes is evident from the higher values of mixed currents and the more negative mixed potentials.

During long-term kinetic tests of the investigated catalysts in an aerated alkali solution of Na₂S, it has been found that the mean reaction rate values determined by the two methods are comparable - Table 15.

Table 15. Oxidation rate values of sulfides on NiW catalysts determined by electrochemical and catalytic experiments.

Catalyst type	Electrochemical rate, mmol/l.h	Catalytic rate, mmol/l.h
NiW _{high} /Ni-foam	1.55	1.78
NiW ₁₀ /Ni-foam	1.74	1.80

After the catalytic experiments conducted, the surface of both types of catalysts has been covered with an uneven spongy layer, where large amounts of sulfur are detected by Energy Dispersive Spectroscopy (EDS). The conducted X-ray analysis (XRD) strongly confirms the presence of orthorhombic sulfur, demonstrating that sulfide oxidation proceeds to elemental sulfur on the catalysts under investigation.

Similar experiments are carried out with electrodeposited NiMoW/Ni-foam catalysts. The results obtained by both electrochemical and catalytic methods show that the partial replacement of W with Mo leads to a reduction of the catalytic activity for sulfide oxidation [98]. Calculated values of the reaction rate from the mixed current (0.43 mmol/l.h) and the depletion of the sulfides in the catalytic experiments (0.54 mmol/l.h) are comparable to each other but are more than 3 times smaller than those achieved with NiW/Ni-foam catalysts.

The established electrochemical oxidation mechanism of sulfides on the investigated electrodeposited catalysts is the basis for their further testing as anode electrocatalysts in sulfide fuel cells.

II. BIOELECTROCHEMICAL SYSTEMS FOR ELECTRICITY GENERATION AND HYDROGEN PRODUCTION

In this dissertation, results with fundamental and applied character are presented, related to the development and testing of five bioelectrochemical systems, differing by the type of biocatalysts used and their potential application.

II.1. Yeast-based biofuel cells

Biofuel cells using pure cultures are used as model systems to analyze intracellular processes, extracellular electron transfer mechanisms, and optimum conditions for the current generation processes. As most studies in the field are conducted with pure bacterial cultures, the contribution of our scientific group is the development of biofuel cells using eukaryotic cultures - yeasts. Research conducted in the period from 2014 until now is deepened in the study of changes in yeast metabolism under specific conditions by using biofuel cells as a unique instrumentarium.

II.1.1. Mitochondrial origin of electrons involved in EET

By purposeful blocking of the mitochondrial functions of *C. melibiosica* yeast during their cultivation in a biofuel cell by inhibition of complex III of the electron transport chains (ETCs) with the addition of antimycin A, a significant decrease in the generated current and power is established (Figure 66). The relative decrease in the quantity of electricity of $38.8 \pm 1.9\%$ in the presence of antimycin A is very close to the share of the aerobic oxidation processes in the yeast culture compared to the fermentation (about 40:60) determined by the amount of ethanol produced in aerobic and anaerobic conditions.

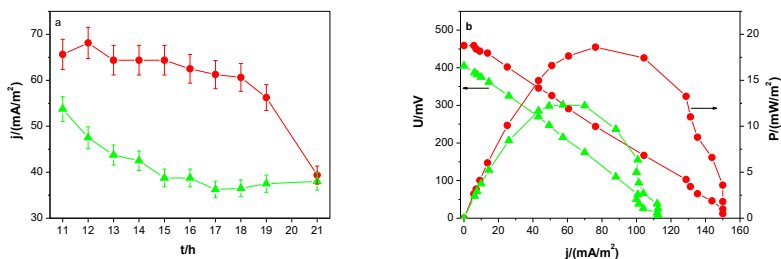


Fig. 66. Electrochemical characterization of a yeast-based biofuel cell with *C. melibiosica* biocatalyst in the presence (Δ) and absence (\bullet) of $30 \mu\text{M}$ of antimycin A as an inhibitor: a) change of the current density over time; b) polarization curves and power curves taken at the 15th hour.

The decrease in the quantity of electricity in the presence of antimycin A is associated with the reduced number of electrons originating from the oxidation of the electronophores (NADH at complex I and FADH_2 at complex II) in the total EET. With the addition of rotenone as a specific inhibitor of I complex, there is less reduction in the quantity of electricity ($25.7 \pm 1.3\%$) as rotenone did not completely block ETC and the electrons supplied in the quinone pool are derived from FADH_2 . The difference in the established quantity of electricity in the presence of the two inhibitors represents the share of the electrons entering ETCs through complex II in the EET processes.

In the presence of the two inhibitors, the COX activity of the corresponding mitochondrial fractions decreases with two orders of magnitude compared to the control. The effect of blocking the electron transfer with antimycin A leads also to a drastic reduction in NADH dehydrogenase activity, probably due to total mitochondrial dysfunction.

The electrochemical activity of the mitochondrial fraction of yeast cultivated in the absence of inhibitors is characterized by the presence of two distinct anodic peaks at potentials of $+0.33$

and +0.70 V (vs. Ag/AgCl) and one cathodic peak at +0.03 V (vs. Ag/AgCl) in the corresponding cyclic voltammogram (Figure 67). The cathodic peak and the anodic peak at +0.70 V are identical to those of reduced cytochrome *c* used as a standard (Fig. 67 – inner graph), i.e. they correspond to the reduction and oxidation of cytochrome *c*.

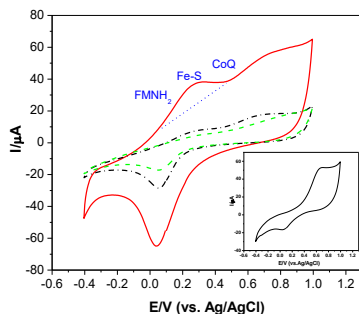


Fig. 67. Cyclic voltammograms of mitochondrial fractions obtained in the absence of inhibitor (solid line), in the presence of rotenone (dashed line) and antimycin A (dotted line); inner graph: CV of reduced cytochrome *c* as a standard.

The drastic reduction of the first anodic peak (at +0.33 V) in the presence of rotenone as compared to the uninhibited mitochondrial ETC suggests that this peak is associated with the electron transfer of reduced flavin mononucleotide (FMNH₂) through the Fe-S clusters of complex I to ubiquinone (CoQ). The disappearance of the two anodic peaks in the presence of antimycin A can be attributed to the total blocking of the electron transfer through ETC in this case. At the same time, in the presence of inhibitors, the electrical outputs of the biofuel cell decrease and become comparable to those reached under strictly anaerobic conditions. The data obtained proves that electrons originating from energetically more favorable processes in yeast mitochondria contribute to increased extracellular electron

transfer and, respectively, to higher electrical current under aerobic conditions.

II.1.2. Influence of newly synthesized redox active dyes on cell metabolism and EET

Searching for new substances that have a positive effect on the processes related to intra- and extracellular electron transfer, newly synthesized styrylquinolinium dyes [219, 220], containing a conjugated bridge (-CH=CH-) linked to two terminal functional groups - a naphthyl group acting as an electron donor, and a quinoline moiety containing quaternary nitrogen acting as an electron acceptor, have been investigated. The potential use of such substances as exogenous mediators in biofuel cells and cell metabolism modulators has not been investigated so far.

II.1.2.1. Styrylquinolinium dye 4-{(E)-2-[4-(dimethylamino)naphthalen-1-yl] ethenyl -1-methylquinoline iodide (DANSQI)

After detailed spectrophotometric and electrochemical characterization under abiotic conditions, the dye has been tested as a potential exogenous mediator in a yeast-based biofuel cell. Immediately after the addition of DANSQI to the yeast suspension (anolyte) a significant shift of the anodic potential in a negative direction and higher values of the generated current are recorded. The increased current values in the presence of the dye are associated with an easier charge transfer (lower activation losses) across the anolyte/anode boundary, supported by the decrease in polarization resistance, recorded by electrochemical impedance spectroscopy (EIS) (Figure 73a).

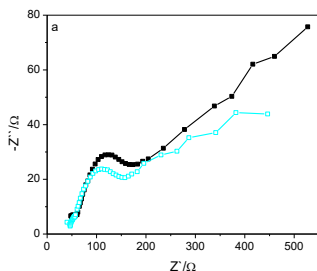


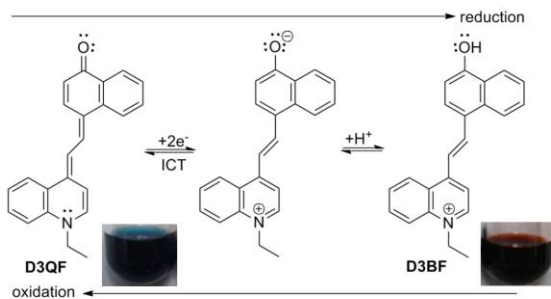
Fig.73. Nyquist plots of yeast suspension before (squares) and immediately after addition of $1 \mu\text{M}$ DANSQI (dots).

In order to clarify the impact of DANSQI on yeast metabolism, two key enzymes - catalase and cytochrome *c* oxidase (the specific enzymes of peroxisomes and mitochondria, respectively) in subcellular yeast fractions, as well as the potential interaction of the dye with the synthesized by yeasts under polarization conditions endogenous mediator (EnM) of electron transfer, are investigated. The analysis of the results of the complex study shows that DANSQI can participate in a number of reversible processes involving the exchange of electrons and/or protons, which in turn affects the mechanism of extracellular electron transfer and the behavior of the studied yeast-based biofuel cell through different stages of its operation. The initially increased values of the generated current are an indication of the enhanced transfer of electrons to the anode. The determined increased catalase activity of a 25% organelle density-gradient fraction in the presence of DANSQI indicates that the dye penetrates the yeast cells, stimulating peroxisome biogenesis. In the interior of the yeast cell the cationic radicals of dye are reduced by the cytoplasmic NADH, which is thermodynamically possible because its formal potential (+0.15 V vs. SHE) is more positive than the redox potential of the pair NAD^+/NADH (-0.32 V vs. SHE), which defines NADH as a

stronger reducer [207, 227]. This hypothesis is supported by the results of CV experiments, which show that NADH and DANSQI can interact *in vitro*. By taking two electrons from NADH, DANSQI becomes a quinoyl radical anion. The protonation of the radical anion is probably synchronous with electron transfer to a suitable intracellular acceptor. By carrying out intramolecular charge transfer and delivering electrons/protons to intracellular acceptors, the dye can play an intracellular shuttle role linking cytoplasmic metabolic processes with mitochondrial ones. The documented increased COX activity and increased values of the generated current by the yeast-based biofuel cell support a similar hypothesis.

II.1.2.2. *Styrylquinolinium dye 4-(E)-1-ethyl-4-(2-(4-hydroxynaphthalen-1-yl)vinyl)quinolinium bromide (D3)*

The styrylquinolinium dye D3 has the same chromophore as DANSQI but at the same time the more reactive donor phenolic hydroxyl group and an ethyl group at the quinoline nitrogen. Initial studies have shown that D3 is an electrochemically active dye and can be converted reversibly from a reduced (benzoid) to an oxidized (quinoid) form (Scheme 4). Besides the type of solvent, the equilibrium between the two forms also depends on the pH of the medium.



Scheme 4. Mechanism of reversible redox conversion of D3.

It is found that the dye formed a tightly adherent coating on carbon felt electrodes when cyclic voltammetry with repetitive cycles has been performed (Figure 79).

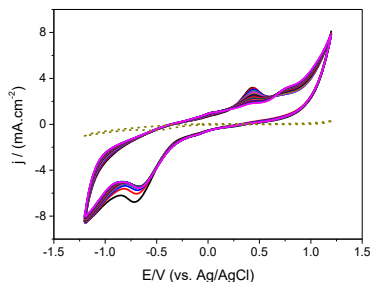


Fig. 79. Cyclic voltammograms of D3 in PBS, pH 7.0, 20 cycles, scan rate 50 mV/s, compared to a CV of unmodified carbon felt (dashed line) in the same solution.

In view of the electrochemical activity of the dye and possible applications of the electrodes thus modified, the electrodeposits obtained are characterized by various methods. By atomic-force microscopy (AFM), it is documented that the electrodeposit on the carbon felt has a well-ordered layered structure (Figure 80).

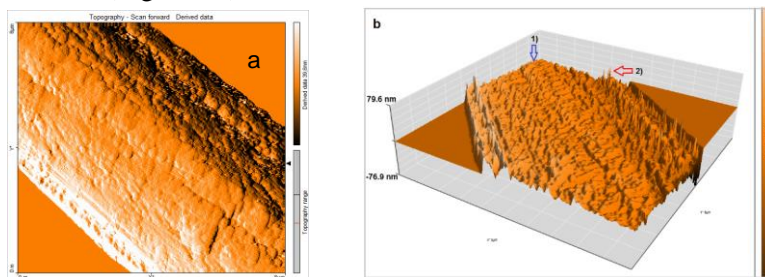


Fig. 80. AFM images of: a) D3-carbon felt (2D); b) D3-carbon felt (3D).

Evidence that the electrodeposits contain predominantly dye monomers are obtained by ESI-MS/MS and the identity of the

deposited organic material is confirmed by NMR. It is assumed that the electrodeposit is stabilized by additional interactions (electrostatic, van der Waals forces, π - π arrangement, etc.) between the planar molecules of the dye.

Based on the idea that the dye in its oxidized form (D3QF) can exchange electrons with suitable electron donors, EIS experiments with modified (D3MED) and unmodified electrodes are performed in the presence of NADH (Figure 83).

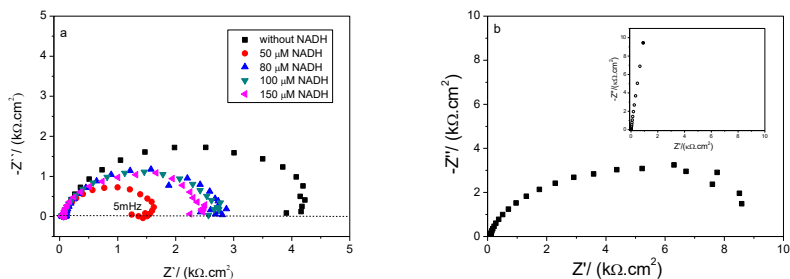


Fig. 83. Nyquist plots of: a) D3MED in PBS with addition of 50 μM NADH (circles), 80 μM NADH (triangles), 100 μM NADH (triangles down), 150 μM NADH (diamonds), control without NADH (squares); b) unmodified carbon electrode as a control in the presence of 80 μM NADH in PBS, internal graph - without NADH.

The resulting impedance spectra are well comparable to an equivalent electric circuit model corresponding to a two-stage electrochemical reaction with the formation of an adsorbed intermediate product (Figure 84). From the calculated data based on this model, it can be concluded that the adsorption resistance, R_{ads} , contributes to the greatest extent to the impedance of the studied system, while the other electrical components (R_{ohmic} , R_{CT} , C_{dl} , C_{ads}) have less impact and relatively close values at different concentrations of NADH. Since, in the applied equivalent model, R_{ads} reflects the contribution of the surface coating from the adsorbed intermediate [229], its almost double less value at 50 μM NADH suggests that at this concentration no saturation of

this coating is achieved, whereas the near R_{ads} values at all higher concentrations suppose that the surface coating reaches a maximum at $80 \mu\text{M}$ NADH.

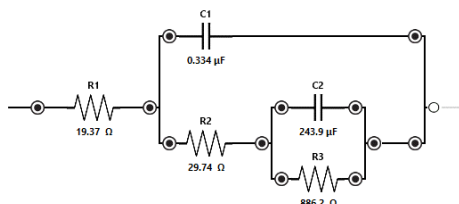


Fig. 84. An equivalent electric circuit model corresponding to a two-stage electrochemical reaction with the formation of an adsorbed intermediate with calculated values of the individual components of the EIS spectrum obtained with D3MED electrode in the presence of $50 \mu\text{M}$ NADH.

The electrocatalytic properties of D3MED with respect to NADH oxidation are also investigated by CV. The shift of the peak potentials in the negative direction as well as the increase of the cathodic peak intensity with the increase of NADH concentration imply the interaction of the electron donor with the oxidized dye molecules (D3QF) on the surface of the electrode. At NADH concentrations above $80 \mu\text{M}$, the height of the cathodic peak ceases to increase, which supports the assumption that the electrocatalytic NADH oxidation is limited by the capacity of the electrodeposition to receive electrons.

The manufactured D3MED electrodes are also tested as anodes in *C. melibiosica*-yeast biofuel cell operating at constant load resistance in a batch mode. The behavior of D3MED anodes is investigated by CV and EIS and compared to that of unmodified carbon anodes as a control.

The results obtained show that the electrodeposition of D3 dye on the carbon felt improves both the kinetics and the

thermodynamics of the anodic half-reaction, which is a prerequisite for practical application.

II.1.3. Influence of polarization on the anabolic activity of the biocatalyst

Although acetate is widely used as a substrate in microbial fuel cells, the processes of its assimilation and dissimilation in living cells used as biocatalysts are not well studied and need further clarification.

The ability of *C. melibiosica* 2491 yeast for carbohydrate biosynthesis from acetate has been studied under conditions modifying cellular metabolism, including polarization of a biofuel cell, lack of carbohydrates and feedback inhibition. Yeast cultivation has been conducted in parallel in three biofuel cells differing in the composition of the culture medium (anolyte) as follows: acetate with the addition of carbohydrate (YBFC₁), acetate only (YBFC₂), and acetate with the addition of malate as a competitive product inhibitor of the glyoxalate cycle enzymes (YBFC₃).

The highest currents, respectively, the quantity of electricity passing through the BES, are recorded with the biofuel cell YBFC₂, while with YBFC₁ it is ~ 35% less. At the same time, the addition of 10 mM malate to the yeast suspension (YBFC₃) leads to a reduction in the quantity of electricity by ca. 55%.

EIS analyzes have shown that the diffusion hindrances and the charge transfer resistance are the smallest in YBFC₂ (Figure 92), which corresponds to the highest values of the quantity of electricity generated by this biofuel cell.

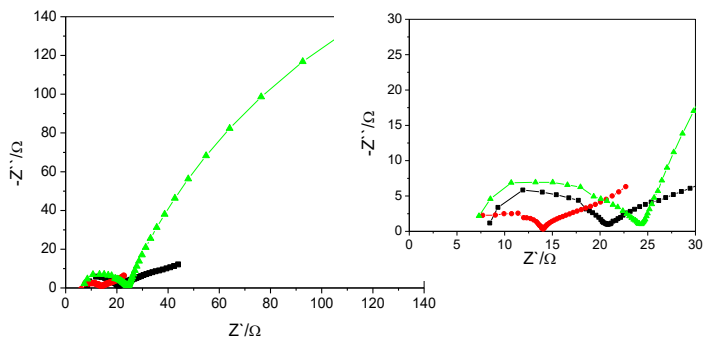


Fig. 91. Nyquist plots obtained by EIS analyzes of the analytes used in YBFC₁ (squares); YBFC₂ (circles); YBFC₃ (triangles). Right graph - magnification of the high-frequency region.

The CV results (Figure 92) show that well-shaped anodic and cathodic peaks appear in the voltammograms obtained with the analytes from YBFC₁ and YBFC₂ at potentials consistent with those of the endogenous mediator, established in previous studies [205-207]. In the presence of carbohydrate in the culture medium (YBFC₁), both peaks are significantly lower than those of the fructose-free sample (YBFC₂), which illustrates a difference in cellular redox activity of the yeast. Yeast suspensions cultivated in the presence of an inhibitor (YBFC₃) or without polarization (control) do not exhibit electrochemical activity.

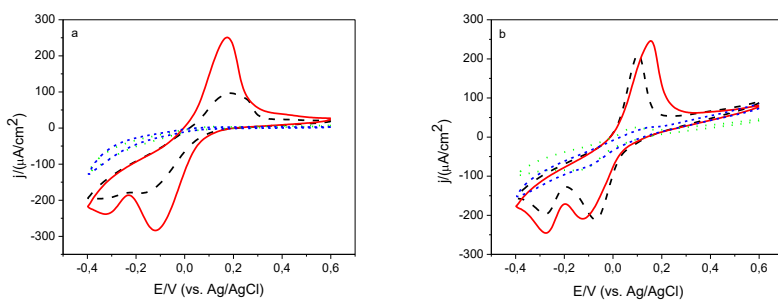


Fig. 92. Cyclic voltammograms of: a) yeast suspensions; b) cellular-free fractions obtained by centrifugation of the yeast suspensions cultivated in acetate buffer: YBFC₁ - in the presence of carbohydrates (dotted line); YBFC₂ - acetate alone (solid line); YBFC₃ - in the presence of malate as an inhibitor (dashed line) and control - acetate, without polarization (short dashed line).

The analysis of the content of reducing sugars in the cultivation medium reveals potential differences in yeast metabolism. Within the cultivation under polarization and presence of carbohydrate source (YBFC₁), 0.575 ± 0.029 g/L, representing about 20% of the initial fructose, is assimilated. Despite the absence of carbohydrates in the starting medium, detectable quantities of reducing sugars are also found in the remaining samples. Considering that in these samples acetate is the only carbon source in the starting medium, the appearance of carbohydrates at the end of cultivation can be explained by the involvement of the glyoxylate pathway in yeast metabolism. The highest intracellular malate dehydrogenase (MDH) activity has been determined for the YBFC₂ sample. The 24-fold lower MDH activity of the YBFC₃ fraction is an indication that the malate acts as a product inhibitor.

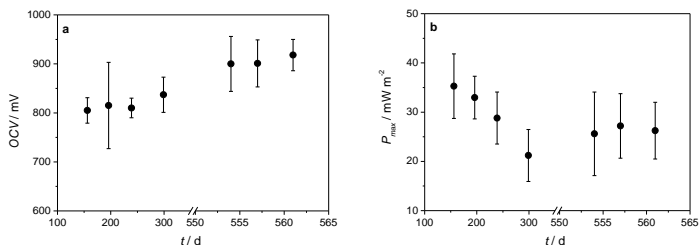
The results of the conducted complex studies show that at applied polarization and the lack of a carbohydrate source the glyoxylate cycle is activated in the yeast cells. The high electrical outputs obtained during yeast cultivation in the acetate medium, along with the highest MDH activity, demonstrate the contribution of the glyoxylate pathway to EET in the bioelectrochemical system.

II.2. Sediment microbial fuel cells - mixed bacterial communities as biocatalysts in the electrochemical system

Most sediment microbial fuel cells (SMFCs) have been studied using marine sediments and water, due to the high salinity, resp. the electrical conductivity of seawater. In view of the relatively small number of publications, our interest is mainly focused on the exploration of SMFCs using sediment from freshwater sources. Different constructions of laboratory and field SMFCs have been developed, some of which have been tested for more than 5 years.

II.2.1. Operational characteristics for long-term operation of SMFCs using freshwater sediments

In long-term trials of nine identical SMFCs operating autotrophically with sediment and water samples from the same freshwater source, it is found that after a certain adaptation period there is a synchronization in the behavior of individual SMFCs, expressed in the same trends in the change and reaching a steady state of the electrical parameters (Figure 110).



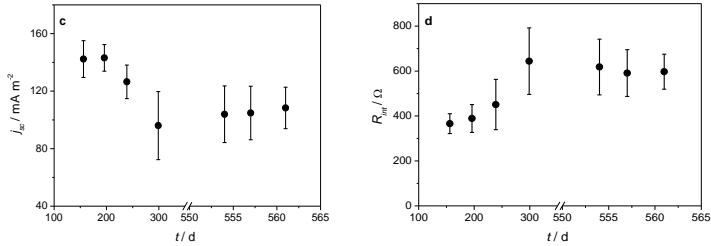


Fig. 103. Most probable values and corresponding uncertainties of the electrical parameters obtained during the operation of nine identical SMFCs: a) OCV; b) maximum power density; c) short-circuit current density; d) internal resistance of the system.

No correlation has been established between the values of current generated by SMFCs and the heavy metal content in the sediments as well as the other physicochemical parameters (pH, temperature, and conductivity) of samples from nine water sources.

During the adaptation period, all of the studied SMFCs experienced visual changes (similar to those of the Winogradsky column) related to the redistribution of bacterial species according to the concentration gradients in the sediment layer. With the appearance of photosynthetic bacterial colonies, a periodic oscillation of open-circuit voltage (OCV) and the generated current begins, following the day-night cycle (Figure 109).

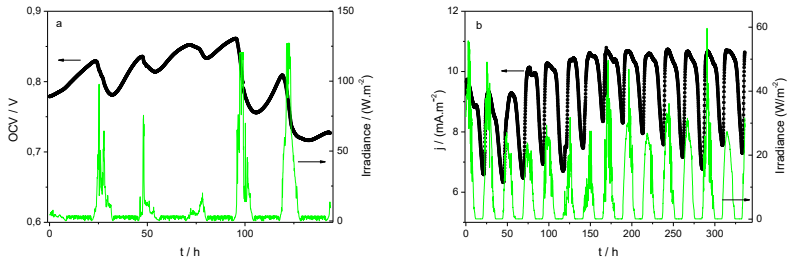


Fig. 109. Variation of: a) OCV; b) the current density generated by SMFC by changing the intensity of illumination within several days.

At controlled temperature and light irradiation, the generated current by SMFC increases, while at darkness the current decreases (Figure 111).

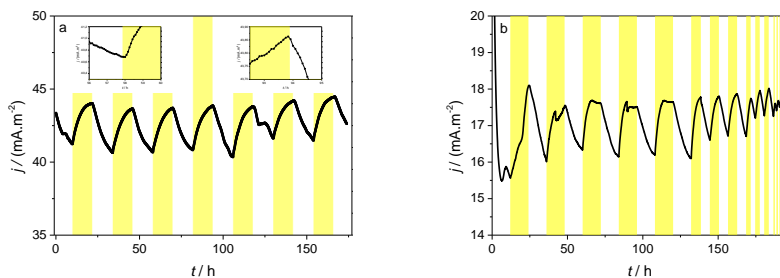


Fig. 111. Change in current density when applying light-dark cycles: a) with a photoperiod duration of 12 hours; b) with decreasing duration of the photoperiod from 12 to 1 h.

Since the SMFC anodes are placed deep in the sediment layer, the hypothesis is raised that the influence of light on the generated current is related to phenomena occurring near the cathode (Figure 114). The catalytic effect of the cathode biofilm on the reduction half-reaction is established by comparing the data from polarization experiments carried out with SMFCs working with an abiotic or biotic cathode (Figure 115). The more positive open circuit cathodic potential (OCP) in the presence of biofilm favors the achievement of a higher electromotive force, and the three-fold higher exchange current density calculated from the linear voltammograms is indicative of enhanced kinetics of the cathodic reaction.

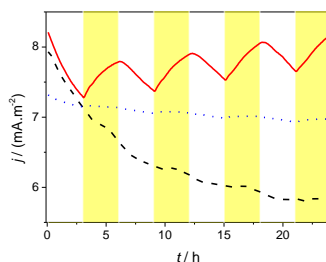


Fig. 114. Variation of the current density at an illumination of the SMFC with a photoperiod duration of 3 hours and the use of a cathode: with formed biofilm (solid line); coated with nontransparent foil (dashed line); new, without biofilm (dotted line).

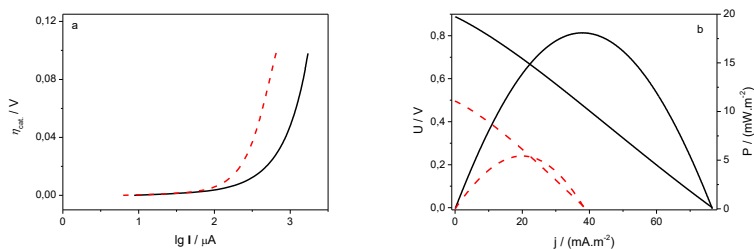


Fig. 115. a) Linear voltammograms presented as Tafel plots; b) polarization curves and power curves obtained with SMFC, operating with a cathode with biofilm (solid line) and cathode without biofilm (dashed line).

When irradiating SMFCs with monochromatic sources covering the entire spectrum of visible light, distinct response to certain wavelengths is established (Figure 117). The greatest impact on the current increase is achieved by irradiation at 665 nm, followed by those at 620 nm and 447 nm. Wavelengths 665 and 447 nm are very close to those of the characteristic absorption peaks of chlorophyll *a* [262], which is the most important pigment in the photosystem of oxygen photosynthesis, whereas 620 nm is associated with the absorption maxima of phycocyanin - additional antenna pigment in cyanobacteria

photosystems that promote a more efficient absorption of light energy [263].

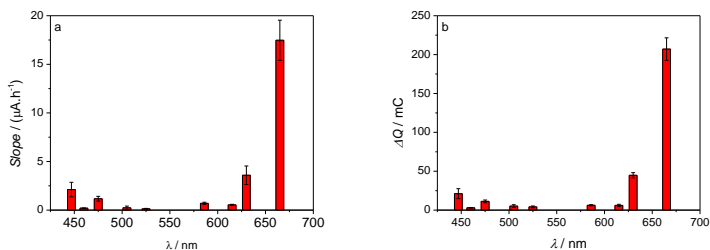


Fig. 117. a) Rate of response to illumination; b) an increase in the quantity of electricity generated during photoperiods, recorded during irradiation of SMFC with monochromatic light of different wavelengths.

The results show that the increased currents during photoperiods are associated with photosynthetic processes running on the SMFC cathode. We suppose that *in situ* bio-oxygen produced by photosynthetic microorganisms in the cathode biofilm consortium reduces transport hindrances for the reduction of oxygen (ORR), thus improving the kinetics of cathodic semi-reaction.

II.2.2. Identification of the SMFC microbiome

The investigation of microbial diversity in SMFC is of utmost importance in view of both better understanding of electron transfer mechanisms and of the possibilities of optimizing the operation of SMFCs and scaling-up them from laboratory type reactors into real-life devices with multiple applications.

After serial dilution and sieving in specific media of samples from the water-sediment column and the two electrodes of SMFC, the total DNA is isolated from the grown up colonies and after the subsequent procedure including PCR amplification of 16S rRNA and sequencing, the types of the isolated

microorganisms are determined. Of 55 colonies of microorganisms, 19 species have been identified. Among them, bacteria of the genera *Clostridium*, *Pseudomonas* and *Bacillus* have proven exoelectrogenic properties. For the first time bacteria of the genera *Lysinibacillus* and *Paenibacillus* are identified from the anodic biofilm, making them potential candidates for the list of exoelectrogenic species from freshwater sediments.

Extremely rich variety (711 species of prokaryotes and 1445 types of eukaryotes) has been found by metagenome analysis of a cathodic biofilm sample (Figure 125). Among the variety of bacterial species, the presence of cyanobacteria, whose unique ability to perform oxygen photosynthesis, is proven to be the most likely reason for established photoinduced fluctuations of SMFC-generated electric current.

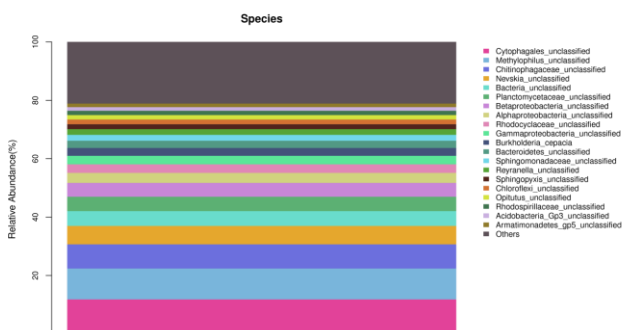


Fig. 125. Taxonomy of bacterial species in the cathodic biofilm of SMFC.

II.2.3. Possible applications of SMFCs as power sources for various devices

In view of the possibilities for powering of commercial electric devices, tests with stacks of SMFCs connected in series or in parallel are performed (Figures 130 and 131).

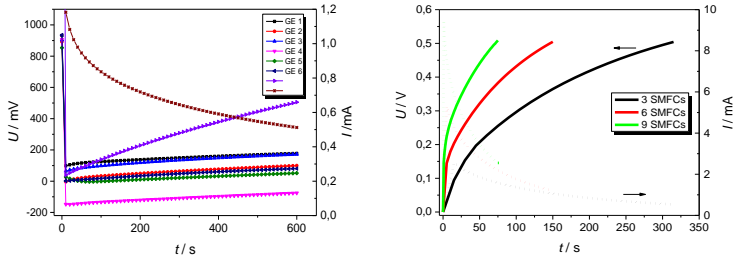


Fig.130. Voltage recorded by six connected in series SMFCs charging a 1F supercapacitor. (left)

Fig. Registered current and voltage in charge mode of a 1F supercapacitor by 3, 6 or 9 parallel-connected SMFCs. (right)

The results show that with a proper connection of several SMFCs in a stack, electrical outputs sufficient to supply low power devices can be achieved (Figure 132).



Fig. 132. Powering a meteostation by 6 SMFCs connected in series.

Studies have been also carried out on the possibility of using SMFCs as autonomous power supplies at field conditions. For this purpose, two 50 liters SMFCs of the same design and anodes of granular graphite and metallurgical coke are constructed. An automated system for eco-monitoring, powered by field SMFCs, has been developed by using an ultralow power management unit and a module with integrated sensors for measuring relative humidity, temperature, illumination, UV index, atmospheric

pressure, concentration of carbon dioxide and volatile organic compounds, sending data to a personal computer or a mobile device.

The collected results from the long-term ecological monitoring are subjected to a regression analysis, which seeks a correlation between the measured environmental parameters and the generated current by the explored SMFCs. The analysis carried out shows that except the light (Figure 146), the other environmental parameters have a negligible influence on the behavior of SMFCs, which in turn leads to relatively persistent electrical characteristics over time under certain operating modes.

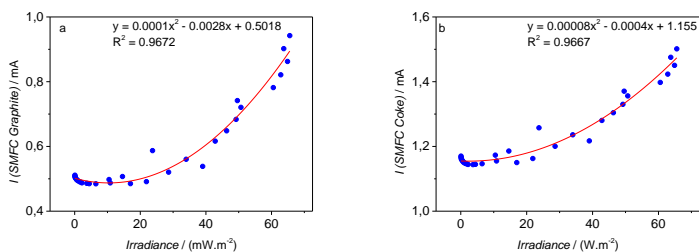


Fig. 146. Dependence of the generated current (mA) on the illumination ($\text{W}\cdot\text{m}^{-2}$) of the fuel cells being studied.

II. 3. Direct Photosynthesizing Plant Fuel Cells

Among the newest types of X-MFC are plant microbial fuel cells (P-MFCs), which operate on the basis of mutualism between the plants and soil microorganisms in the rhizosphere. In our previous studies [284, 285], it has been reported that higher aquatic plants - *Lemna minuta* and *Lemna valdiviana* - can be used as biocatalysts in Direct Photosynthesizing Plant Fuel Cells (DPPFC) without the involvement of any exoelectrogenic bacteria. For a more detailed examination of the influence of light on the electrical outputs of DPPFC, a special experimental setup

has been developed to allow irradiation of plants with mono- and polychromatic polarized light. *Lemna minor* duckweeds are used as a biocatalyst in the experiments.

Immediately after irradiation of the plants with polarized red or blue-violet light, the generated current increases and with slight fluctuations is stable up to 3 hours (Figure 152a). Periodic exposure to red light results in the highest values of current density. The wavelengths of 650 and 450 nm are close to those of the characteristic absorption peaks of chlorophyll *a* and *b*, which are the most important pigments in green plant photosystems. The results of the measurements show that the polarized polychromatic light influences faster and to a greater extent on the generated current compare to the non-polarized light (Figure 152b).

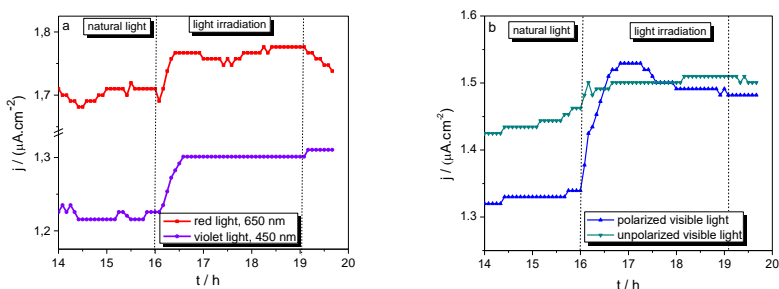


Fig. 152. Current density measured during irradiation of PPFC with: a) red and violet light; b) polarized and non-polarized visible light.

The obtained impedance spectra indicate that the system reacts differently depending on the applied irradiation. While the spectra of PPFC1 (monochromatic red light) and PPFC4 (non-polarized visible light) are well suited to the Randles model for one-time constant (Figure 154a), PPFC2 and PPFC3 (polarized visible light) corresponds to the equivalent electric circuit model, consisting of two consecutive RC time constants (Figure 154b). Based on the similarity between the impedance spectra of PPFC1

and PPFC4, it is supposed that complexes of plant photosensitive systems capable of absorbing red light can contribute to the direct transfer of electrons from the leaves through the roots of the duckweeds to the anode of the fuel cells.

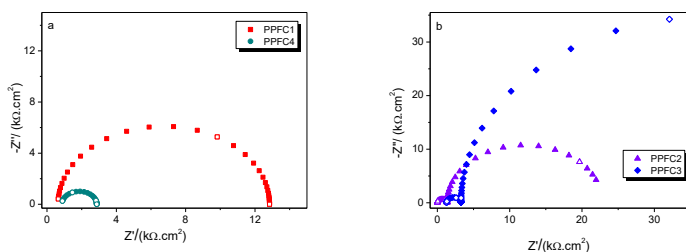


Fig. 154. EIS of bioanodes during irradiation presented as Nyquist plots: a) PPFC1 (squares) and PPFC4 (circles); b) PPFC2 (triangles) and PPFC3 (diamonds).

II.4. Regeneration of metals combined with wastewater treatment in microbial fuel cells

Bioelectrochemical systems, in which bio-catalyzed anode oxidation of substrates can be combined with the reduction of diverse electron acceptors, offer a new alternative for the recovery of metals from wastewater without the need for preconcentration. In the dissertation, results, illustrating the principal possibility of developing MFC technology for the simultaneous electric current generation, copper recovery and wastewater purification from biodegradable organic matter, are presented. The experiments are conducted in double-chamber fuel cells. As an anolyte, synthetic wastewater is used, to which activated sludge from the municipal wastewater treatment plant – Blagoevgrad is added, and as catholytes CuSO_4 solutions with different initial concentration have been used.

Direct evidence of the formation of an electroactive biofilm and its key role in the overall behavior of the system is the change

of the generated current over time (Figure 158), which in all experiments carried out strictly follows the changes of the anodic potential. The electrical current from the abiotic fuel cell (K3) is negligible and does not change over time.

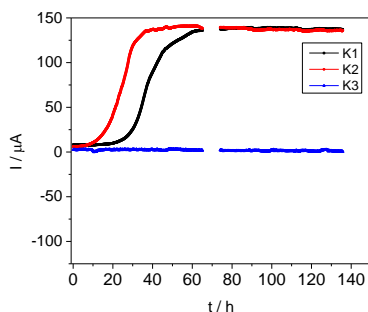


Fig. 158. Generation of electric current from microbial fuel cells using 0.1 M CuSO_4 as a catholyte over time.

When using biotic anodes, elemental copper is deposited on the MFC cathodes, the quantity of which is determined by weight analysis after each experiment. The influence of Cu^{2+} ions as the final electron acceptor on the behavior of the BES studied is more noticeable when using the most concentrated catholyte (0.1 M CuSO_4). In addition to generating more electricity and more deposited copper on the cathode, the higher amperage accelerates the formation of the anodic biofilm, resulting in a more stable and reproducible behavior of the system over time.

The efficiency of the processes carried out in the system is evaluated by the copper regeneration rate, η_{Cu} , calculated as the mass ratio of the copper deposited on the cathode to the copper mass in the starting solution, as well as the percentage reduction of COD in the anolyte, η_{COD} , which serves as a measure for wastewater treatment. Despite the higher amounts of copper deposited, the degree of regeneration by the highest concentration

(0.1 M CuSO₄) of catholyte is the lowest, whereas at a 20-fold dilution of the stock solution η_{Cu} increases more than 10 times - Table 34.

Table 34. Copper regeneration rate using CuSO₄ solutions of varying concentrations as catholyte in MFC.

MFC	$\eta_{\text{Cu}} / \%$		
	0.1 M CuSO ₄	0.01 M CuSO ₄	0.005 M CuSO ₄
K1	3.1	20.2	43.4
K2	3.0	15.1	30.2

On the other hand, in most experiments, the COD decreases by half, with no correlation between this indicator and the electrical characteristics or concentration of Cu²⁺ in the catholyte. This result indicates that dominating in substrate degradation are microorganisms other than the exoelectrogenic ones responsible for EET, respectively, for the current generation in the system.

The performed study confirms the possibility of developing a MFC-based technology for simultaneous purification of biodegradable organic products and regeneration of copper from wastewater, which additionally generates electricity.

II.5. Microbial electrolysis cells

One of the latest technologies for hydrogen production, developing only for a decade, is the so-called microbial electrolysis. An advantage of microbial electrolysis is that, due to the use of bioanode, the theoretical voltage required to generate hydrogen on the cathode is significantly less than that (1.23 V) for conventional water electrolysis [304, 305]. Another advantage is that along with the production of hydrogen, biodegradable waste products are purified simultaneously. As far as MECs use identical

bioanodes with those in MFCs, the main challenge for their practical application as a hydrogen production technology is to find cathode catalysts with low cost and sufficient efficiency.

II. 5.1. New electrocatalysts for application in MEC

Synthesized and tested as potential cathode electrocatalysts for MECs are over 20 nanocomposite materials, not containing precious metals, as well as Pd-Au nanocomposites with different contents of the two metals. The produced materials are classified into the following 4 groups:

- 1) CoB, NiB, and CoNiB;
- 2) NiMo and NiW;
- 3) NiFe, NiFeP and NiFeCoP;
- 4) PdAu.

The morphology of the obtained materials is characterized by scanning electron microscopy (SEM), and by EDS analysis the presence of the corresponding chemical elements in the depositions is confirmed. Corrosion tests are conducted, from which the values of corrosion potential and corrosion current for all modified electrode materials are calculated. The highest corrosion resistance exhibits NiW and NiMo composites, with corrosion rates for depositions on nickel-foam being 3 orders of magnitude lower than those on carbon felt.

The electrocatalytic activity of the modified materials with respect to the hydrogen evolution reaction is investigated and compared with that of the unmodified substrates by linear voltammetry and chronoamperometry. From the voltammograms obtained, the potential at which the hydrogen evolution begins, V_e , and the slope of the steep linear cathode region, V_e , as a measure of the HER rate [313], are determined. The analysis of the experimental results shows that the overpotential of hydrogen evolution on all modified electrodes, with the exception of the

deposits obtained by chemical reduction on nickel foam, is smaller than that of the unmodified materials used as supports. The most significant (over 450 mV) is the reduction of the overpotential at the PdAu/C-felt electrodes. For most of the electrodeposited catalysts, the HER rate, evaluated by V_h , increases compared to unmodified electrodes, whereas for chemically deposited catalysts the V_h values are close to those of the support. For PdAu-modified electrodes, there is a tendency of increase of the HER rate with a decrease in Pd content, more pronounced for samples deposited on nickel foam. The most significant increase in V_h is found for the third group electrodes (NiFe, NiFeP, NiFeCoP), with the highest rates of HER being achieved with NiFeCoP catalysts in both neutral and weakly acidic electrolytes. The hydrogen generation rates in acetate buffer with this group of electrodes exceed 3.3 to 6.5 times those in phosphate buffer. The highest current density of $165 \pm 3 \text{ A/m}^2$ (at -1.0 V vs. SHE) corresponding to a hydrogen production rate of $1.7 \pm 0.1 \text{ m}^3 \text{ H}_2/\text{day/m}^2$ is achieved with NiFeCoP in acetate buffer.

As a method providing results with relatively low uncertainty, mass spectrometry (MS) is used as a reference method for calibrating potentiostatic measurements. For this purpose, experiments with a series of PdAu/C-felt electrodes are carried out, in which applying different cathodic potentials the amounts of evolved hydrogen are analyzed by mass-spectrometer. By integrating the areas under the chronoamperometric curves obtained and applying Faraday's law, the estimated amounts of evolved hydrogen at the various potentials are calculated and compared with those determined by mass-spectrometric measurements (Figure 168).

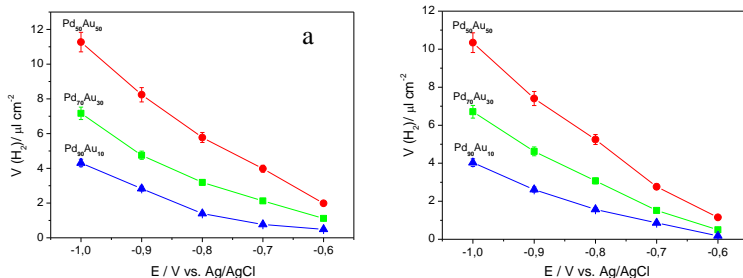


Fig. 168. Quantities of evolved hydrogen at different applied potentials calculated from: a) MS data; b) chronamperometric measurements.

Within the uncertainty of the measurements, the results of both methods are identical for all samples of the test series, which makes it possible to use chronoamperometry as a reliable method for the quantification of electrochemically produced hydrogen, respectively, to investigate the electrocatalytic activity of various electrode materials with respect to HER. Results from chronamperometric measurements, validated by MS, confirm the established by linear voltammetry tendency to increase the electrocatalytic activity of synthesized PdAu nanocomposites with an increase in the Au:Pd ratio.

For catalysts deposited by borohydride reduction on carbon felt, the tendency to increase electrocatalytic activity with a decrease in the Co and an increase in Ni content is confirmed, with NiB samples being most active.

Electrodeposited NiW and NiMo also exhibit a similar but higher catalytic activity than the support, with some priority of NiW catalysts at potentials more negative than -1.1 V. Based on their relatively high catalytic activity, the highest corrosion resistance and the absence of precious metals in their composition,

the catalysts of this group are selected as cathodes for further tests in a microbial electrolyser.

II.5.2. Bioelectrochemical production of hydrogen

Laboratory tests for bioelectrochemical hydrogen production are conducted in a single-chamber microbial electrolysis cell. In the initial tests, cathodes from unmodified nickel foam are used, and as an anodic biocatalyst - a pure bacterial culture of *Lactobacillus plantarum* AC11, proven to be an exoelectrogenic strain in previous studies [314]. The obtained results show that in the presence of a biocatalyst and applied voltage 1V an electric current flows in the system and hydrogen is released on the cathode (Figure 184). With the same strain, no faradaic reaction occurs in the abiotic control (AC-fuel cell, not inoculated with microorganisms), which demonstrates the role of the biocatalyst and confirms the principle of MEC.

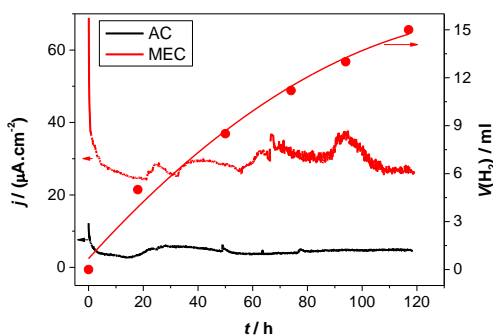


Fig. 184. Change of current density and quantities of produced hydrogen during MEC operation with *Lactobacillus plantarum* AC11 biocatalyst at applied voltage 1V, AC - abiotic control.

Experiments with wastewater and activated sludge (AS) have been also conducted, in which NiW and NiMo electrodeposited on nickel foam are investigated as cathode catalysts in MEC. At the

same applied voltage, the current density in the system is greater with the use of modified cathodes compared to unmodified nickel foam, with higher values being recorded with NiW/Ni-foam cathodes (Figure 185). Moreover, the current density values at an applied voltage of 0.6 V are several times higher than those obtained with the use of a pure bacterial culture at a voltage of 1 V. The contribution of the biological component to the electrolysis performed at voltages <1 V is also proved by control abiotic experiments with wastewater without activated sludge, where it is found that there is practically no current in the system and no release of gaseous products is observed in contrast to the biotic experiments in which, the release of gas on the cathode begins right after applying of external voltage.

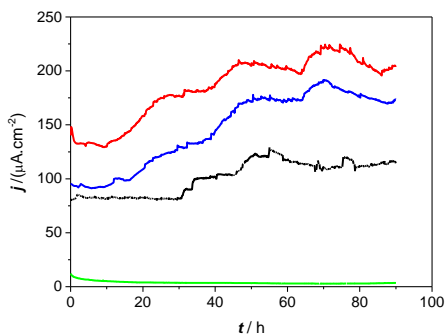


Fig. 185. Variation of the current density during operation of MEC with wastewater and activated sludge from the Wastewater Treatment Plant - Blagoevgrad using NiW/Ni-foam cathodes (red line); NiMo/Ni-foam (blue line); unmodified Ni-foam (black line); abiotic control (green line); U_{app} = 0.6V.

A linear correlation between volumetrically measured amounts of evolved gas and the quantity of electricity passed through the system is established (Figure 186). Since this correlation strictly obeys the Faraday's law, electrochemically

produced hydrogen on the cathode can be considered to be the main gaseous product, which is consistent with results reported by other research groups.

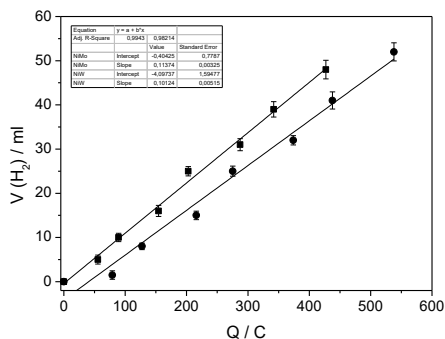


Fig. 186. Correlation between the volume of the produced gas and the quantity of electricity passed through the MEC at 0.6 V applied voltage using NiW/Ni-foam and NiMo/Ni-foam cathodes.

Combining the definition equation for the cathodic hydrogen recovery with the analytical form of the experimentally obtained linear regressions $V(\text{H}_2) = f(Q)$, the following semi-empirical equation for r_{cat} is derived:

$$r_{\text{cat}} = \frac{2FT_0b}{1000V_mT} 100 = \frac{2,36 \cdot 10^5 b}{T}, \%$$

where $F = 96\,485 \text{ C}$ - Faraday constant; $T_0 = 273.15 \text{ K}$; T - working temperature, K; $V_m = 22.4 \text{ l}$ - molar volume of gas under normal conditions; b - linear slope of dependence $V(\text{H}_2) = f(Q)$, $\text{ml} \cdot \text{C}^{-1}$.

The MEC efficiency using the tested cathodes is evaluated by hydrogen production rate, energy efficiency, and cathodic hydrogen recovery. The calculated values for the three parameters are presented in Table 34.

Table 34. Hydrogen production rate, cathodic hydrogen recovery and energy efficiency of MEC using different cathodes.

Cathode	Q_{H_2} , $\text{m}^3(\text{H}_2) \text{m}^{-3} \text{d}^{-1}$	r_{cat} , %	η_{E} , %
NiW/Ni-foam	0.14±0.01	78.9±1.7	205.2±4.7
NiMo/Ni-foam	0.13±0.01	88.6±2.3	238.4±11.3
Ni-foam	0.04±0.00	40.0±1.5	98.4±3.3

The hydrogen production rates achieved with NiW/Ni-foam and NiMo/Ni-foam cathodes exceed 3.5 times that of unmodified Ni-foam, which confirms their higher electrocatalytic activity with respect to HER found in abiotic experiments. Despite the low productivity, the calculated cathodic hydrogen recovery and energy efficiency data obtained with the NiW and NiMo cathodes tested are comparable and even higher than those reported in other studies [316-319]. Whereas, for NiW/Ni-foam cathodes hydrogen production has a higher rate, the calculated r_{cat} for MEC with NiMo/Ni-foam (88.6±2.3 %) is greater than that obtained with NiW/Ni-foam (78.9±1.7 %). Higher values for r_{cat} are also reported for MEC using NiMo/carbon cloth as compared to NiW/carbon cloth as cathodes [317]. The greater amount of electricity input is also the reason for the lower energy efficiency achieved with NiW/Ni-foam (205.2±4.7 %), compared to NiMo/Ni-foams cathodes (238.4±11.3 %). Regardless of NiMo/Ni-foam superiority in terms of cathodic hydrogen recovery and energy efficiency, the higher corrosion resistance of NiW coatings combined with higher productivity is an important advantage for practical application.

CONCLUSIONS

1. The results of the performed complex studies reveal opportunities for the development of new technologies for electricity generation and hydrogen production, based on different (bio) electrochemical systems. In most of the systems studied, there is also a potential for simultaneous wastewater purification without adding extra energy.

2. Metal hydride alloys of AB_5 type are suitable for preparation of anodes for direct borohydride fuel cells (DBFCs). The nanocomposite CoNiMnB-electrodes are appropriate for application in hybrid systems combining direct borohydride fuel cell and Hydrogen-on-demand generator.

3. Soluble sulfides at comparatively low concentrations ($<0.1\text{mol/l}$) can be used as a fuel in fuel cells with liquid anolyte and various cathodic depolarizers, which reveals the possibility of purification of sulfides in wastewater with simultaneous generation of electric current.

4. Along with their primary purpose of generating electricity and wastewater treatment, biofuel cells can serve as a unique tool for exploring the metabolic pathways of microorganisms, participating in the intra- and extracellular electron transfer.

5. Sediment microbial fuel cells can operate autotrophically for years. The cathodic biofilm, containing photosynthetic microorganisms, plays an important role in their performance. Their simple design, the use of cheap and accessible materials, as well as the possibility of increasing the output voltage and current through a connection in stacks or using voltage converters are prerequisites for using SMFCs as cheap autonomous power sources for powering of various electronic devices, e.g. for eco-monitoring in remote and hard-to-reach areas.

6. The light absorbing photosystems (PS I and PS II) and ETC in the thylakoid membranes of duckweeds are involved in the direct electron transfer to the anode.

7. Biofuel cell technology allows the simultaneous regeneration of copper and purification of wastewater from biodegradable organic wastes without adding extra energy and concentration of input streams.

8. NiW and NiMo, electrodeposited on nickel foam, are the most promising cathode catalysts of the 27 newly synthesized materials for use in a microbial electrolysis cell. To increase hydrogen productivity, it is necessary to optimize the design of the MEC reactor, use of suitable exoelectrogenic bacteria to improve the bioanode efficiency, optimize the parameters of the electrolyte (conductivity, COD, pH) and the applied external voltage.

CONTRIBUTIONS

1. Seven new types of electrochemical systems (2 abiotic and 5 biotic) with potential for practical application for the electric current generation and hydrogen production are developed and characterized.
2. Hydrogen-absorbing alloys and composites (three AB₅-type metal hydride alloys and eleven 2-, 3- and 4-component nanocomposites) are studied as anode material for sodium borohydride electrooxidation. Of these, the AKL-86 alloy exhibits the highest discharge capacity in a direct borohydride fuel cell, with two air cathodes achieving a five-fold increase in maximum power.
3. The oxidation of sulfides in fuel cells with different cathodic oxidants, electrode materials, and separators, has been investigated. The established catalytic activity of NiW and NiMoW electrodeposits with respect to the sulfide oxidation in an alkaline electrolyte makes them suitable anode catalysts for alkali sulfide fuel cells.
4. It has been proved that electrons originating from the mitochondrial oxidation processes of the substrate are extracellularly transferred and involved in the current-generating processes in a yeast-based biofuel cell. In acetate, yeasts cultivated under polarization activate the glyoxylate metabolic pathway for synthesis of carbohydrate precursors, contributing to enhanced extracellular electron transfer (EET).
5. It has been established that styrylquinolinium dyes are suitable for use as exogenous EET mediators in a yeast-based biofuel cell. Modified electrodes with enhanced electrocatalytic activity in respect to the anodic semi-reaction are produced by

electrodeposition of 4-(E)-1-ethyl-4-(2-(4-hydroxynaphthalen-1-yl) vinyl) quinolinium bromide dye on a carbon support.

6. Sediment microbial fuel cells (SMFCs) with various design and volume have been developed. In long-term operation in autotrophic mode, the SMFCs demonstrate stable electrical performance, mainly influenced by illumination. It has been proved that the registered increased currents during photoperiods are associated with photosynthetic processes running on the SMFC cathode. The metagenome analysis of a cathodic biofilm demonstrates a wide variety of prokaryotes (711 species), including cyanobacteria capable to carry out oxygen photosynthesis, and eukaryotes (1445 species) coexisting on the cathode surface.

7. The application of on-field operating SMFCs to supply a sensor module for long-term environmental monitoring has been demonstrated.

8. The participation of photosystem I and II of photosynthetic microorganisms and plants in the direct EET to the biofuel cell anode is established.

9. The possibility to create MFC-based technology for simultaneous purification of biodegradable organic wastes and regeneration of copper from wastewater, which additionally generates electric current, has been confirmed.

10. The corrosion resistance and electrocatalytic activity with respect to HER of 27 newly synthesized materials of different composition in neutral phosphate electrolyte are evaluated for potential use as cathodes in a microbial electrolyser. With two types of modified cathode materials - NiW/Ni-foam and NiMo/Ni-foam, higher energy efficiency as well as cathodic hydrogen recovery are achieved compared to those reported in the literature for non-platinum catalysts.

LIST OF PUBLICATIONS, INCLUDED IN DISSERTATION

I. Papers in journals with an impact factor (Overall Impact Factor of included publications 50,811)

1. I. Bardarov, **M. Mitov**, D. Ivanova, Y. Hubenova (2018) Light-dependent processes on the cathode enhance the electrical outputs of sediment microbial fuel cells. *Bioelectrochemistry* 122: 1-10.
DOI: 10.1016/j.bioelechem.2018.02.009 (IF 4.06)
<https://www.sciencedirect.com/science/article/pii/S1567539417306564>
2. Y. Hubenova, R. Bakalska, **M. Mitov** (2018) Electrodeposited styrylquinolinium dye as molecular electrocatalyst for coupled redox reactions. *Bioelectrochemistry* 123: 173–181.
DOI: 10.1016/j.bioelechem.2018.05.006 (IF 4.06)
<https://doi.org/10.1016/j.bioelechem.2018.05.006>
3. Y. Hubenova, E. Hubenova, R. Bakalska, **M. Mitov** (2018) Redox interactions between dye 4-(E)-1-ethyl-4-(2-(4-hydroxynaphthalen-1-yl)vinyl)quinolinium bromide and NAD⁺/NADH. *Bulgarian Chemical Communications* 50D: 68-74 (IF 0.238)
4. Y. Hubenova, E. Hubenova, **M. Mitov** (2018) Chronoamperometrically poised electrodes mimic the performance of yeast-based bioanode. *Bulgarian Chemical Communications* 50D: 62-67 (IF 0.238)
5. Y. Hubenova, G. Ivanov, E. Hubenova, **M. Mitov** (2018) Photo-induced charge transfer between Lemna minor and anode of photosynthesizing plant fuel cell. *Bulgarian Chemical Communications* 50 B: 141-146. (IF 0.238)
6. **M.Y. Mitov**, I.O. Bardarov, E.Y. Chorbadzhiyska, Y.V. Hubenova (2018) Copper recovery combined with wastewater treatment in a microbial fuel cell. *Bulgarian Chemical Communications* 50 B: 136-140. (IF 0.238)
7. **M. Mitov**, E. Chorbadzhiyska, L. Nalbandian, Y. Hubenova (2017) Nickel-based electrodeposits as potential cathode catalysts for

hydrogen production by microbial electrolysis. *J. Power Sources* 356: 467-472.

DOI: 0.1016/j.jpowsour.2017.02.066 (IF 6.395)

<http://www.sciencedirect.com/science/article/pii/S0378775317302409>

8. Y. Hubenova, E. Hubenova, E. Slavcheva, **M. Mitov** (2017) The glyoxylate pathway contributes to enhanced extracellular electron transfer in yeast-based biofuel cell. *Bioelectrochemistry* 116: 10-16.

DOI: 10.1016/j.bioelechem.2017.03.003 (IF 3.346)

<http://www.sciencedirect.com/science/article/pii/S1567539416302390>

9. Y. Hubenova, R. Bakalska, E. Hubenova, **M. Mitov** (2016) Mechanisms of electron transfer between a styrylquinolinium dye and yeast in biofuel cell. *Bioelectrochemistry* 112: 158-165.

DOI: 10.1016/j.bioelechem.2016.02.005 (IF 3.556)

<http://www.sciencedirect.com/science/article/pii/S1567539416300159>

10. **M. Mitov**, I. Bardarov, P. Mandjukov, Y. Hubenova (2015) Chemometrical assessment of the electrical parameters obtained by long-term operating freshwater sediment microbial fuel cells. *Bioelectrochemistry* 106A: 105–114.

DOI: 10.1016/j.bioelechem.2015.05.017 (IF 4.172)

<http://www.sciencedirect.com/science/article/pii/S1567539415000754>

11. Y. Hubenova, **M. Mitov** (2015) Extracellular electron transfer in yeast-based biofuel cells: a review. *Bioelectrochemistry* 106A:177–185. DOI: 10.1016/j.bioelechem.2015.04.001 (IF 4.172)

<http://www.sciencedirect.com/science/article/pii/S1567539415000365>

12. E. Chorbazhiyska, **M. Mitov**, L. Nalbandian, Y. Hubenova (2015) Effect of the support material type on the electrocatalytic activity of Pd-Au electrodeposits in neutral electrolyte. *Int. J. Hydrogen Energy* 40(23):7329–7334 (IF 3.313)

<http://www.sciencedirect.com/science/article/pii/S0360319915008940>

13. Y. Hubenova, **M. Mitov** (2015) Mitochondrial origin of extracellular transferred electrons in yeast-based biofuel cells. *Bioelectrochemistry* 106A:232–239.

DOI: 10.1016/j.bioelechem.2014.06.005 (IF 4.172)

<http://www.sciencedirect.com/science/article/pii/S1567539414000875>

14. **M.Y. Mitov**, G.Y. Hristov, R.S. Rashkov, Y.V. Hubenova (2015) Quaternary electrodeposits on nickel-foam for application in a

hybrid Direct Borohydride Fuel Cell - Hydrogen-on-demand system. *Bulgarian Chemical Communications* 47(4): 995–1001 (**IF 0.349**)

http://www.bcc.bas.bg/BCC_Volumes/Volume_47_Number_4_2015/BCC-47-4-3589-Mitov-995-1001.pdf

15. Y. Hubenova, **M. Mitov** (2015) Application of cyclic voltammetry for determination of the mitochondrial redox activity during subcellular fractionation of yeast cultivated as biocatalysts. *Bulgarian Chemical Communications* 47(3): 821-824 (**IF 0.349**)

http://www.bcc.bas.bg/BCC_Volumes/Volume_47_Number_3_2015/BCC-47-3-Hubenova-821-824.pdf

16. E.Y. Chorbazhziyska, Y.V. Hubenova, G.Y. Hristov, L.Nalbandian, **M.Y. Mitov** (2015) Electrocatalytic activity of Pd-Au co-deposits on Ni-foam towards hydrogen evolution reaction. *Bulgarian Chemical Communications* 47(4): 1002–1007 (**IF 0.349**)

http://www.bcc.bas.bg/BCC_Volumes/Volume_47_Number_4_2015/BCC-47-4-3591-Chorbazhziyska-1002-1007.pdf

17. **M.Y. Mitov**, E.Y. Chorbazhziyska, L.Nalbandian, Y.V. Hubenova (2015) Synthesis and characterization of dip-coated CoB-, NiB- and CoNiB- carbon felt catalysts. *Bulgarian Chemical Communications* 47(3): 825-829 (**IF 0.349**)

http://www.bcc.bas.bg/BCC_Volumes/Volume_47_Number_3_2015/BCC-47-3.pdf

18. **M. Mitov**, Y. Hubenova (2015) Microbial X Cells – Innovative Multipurpose Bioelectrochemical Systems. *Chemistry: Bulgarian Journal of Science Education* 24: 404-416 (**SJR 0.210**)

http://khimiya.org/pdfs/CHEMISTRY_24_3_MITOV.pdf

19. E. Chorbazhziyska, Y. Hubenova, S. Yankova, D. Yankov, **M. Mitov** (2015) *Lactobacillus plantarum* AC 11S as a Biocatalyst in Microbial Electrolysis Cell. *Chemistry: Bulgarian Journal of Science Education* 24: 417-427 (**SJR 0.210**)

http://khimiya.org/pdfs/CHEMISTRY_24_3_CHORBADZHIYSKA.pdf

20. I. Bardarov, Y. Hubenova, **M. Mitov** (2015) Sediment microbial fuel cells as power sources for small electrical consumers. *Chemistry: Bulgarian Journal of Science Education* 24: 433-440 (**SJR 0.210**)

http://khimiya.org/pdfs/CHEMISTRY_24_3_BARDAROV.pdf

21. G. Hristov, E. Chorbadzhiyska, **M. Mitov** (2015) Pd-Au Deposites on Ni-Foam as Anodic Electrocatalysts for Direct Borohydride Fuel Cell. *Chemistry: Bulgarian Journal of Science Education* 24: 424-432 (**SJR 0.210**)
http://khimiya.org/pdfs/CHEMISTRY_24_3_HRISTOV.pdf
22. E. Chorbadzhiyska, **M. Mitov**, G. Hristov, N. Dimcheva, L. Nalbandian, A. Evdou, Y. Hubenova (2014) Pd-Au electrocatalysts for Hydrogen Evolution Reaction at neutral pH. *Int. J. Electrochemistry*, Volume 2014, Article ID 239270, 6 pages (equated due to 9 citations in articles, published in journals with IF)
<http://dx.doi.org/10.1155/2014/239270>
23. G.Y. Hristov, E.Y. Chorbadzhiyska, R.S. Rashkov, Y.V. Hubenova, **M.Y. Mitov** (2013) Comparison investigation of Co-based catalysts for the catalytic hydrolysis of sodium borohydride. *Bulgarian Chemical Communications* 45A: 219-222. (**IF 0.320**)
https://www.researchgate.net/publication/297955597_Comparison_investigation_of_Cobased_catalysts_for_the_catalytic_hydrolysis_of_sodium_borohydride
24. **M. Mitov**, E. Chorbadzhiyska, R. Rashkov, Y. Hubenova (2012) Novel nanostructured electrocatalysts for hydrogen evolution reaction in neutral and weak acidic solutions. *Int. J. Hydrogen Energy* 37(21): 16522–16526. (**IF 4.47**)
<http://www.sciencedirect.com/science/article/pii/S0360319912004661>
25. **M. Mitov**, E. Hristova, G. Hristov, R. Rashkov, M. Arnaudova, A. Popov (2009) Catalytic activity of Ni-W electrodeposits. *Environm. Chem. Lett.* 7 (3): 249-253. (**IF 2.051**)
<http://www.springerlink.com/content/9257276884665516/>
26. **M. Mitov**, G. Hristov, E. Hristova, R. Rashkov, M. Arnaudova, A. Zielonka (2009) Complex performance of novel CoNiMnB electrodeposits in alkaline borohydride solutions. *Environm.Chem.Lett.* 7(2): 167-173. (**IF 2.051**)
<http://www.mendeley.com/research/complex-performance-novel-conimnb-electrodeposits-alkaline-borohydride-solutions/>
27. **M. Mitov**, R. Rashkov, N. Atanassov, A. Zielonka (2007) Effects of nickel foam dimensions on catalytic activity of supported Co-

Mn-B nanocomposites for hydrogen generation from stabilized borohydride solutions. *J. Mat. Sci.* 42: 3367-3372. (IF 2.325)

II. Papers in other specialized journals and proceedings of scientific forums

28. I. Bardarov, E. Chorbadzhiyska, Y. Hubenova, **M. Mitov**. Influence of the physicochemical parameters on the electrical outputs of Sediment Microbial Fuel Cells. In: Proceedings of the PhD Student Scientific Session of the FMNS – 2016, Blagoevgrad, 2016, pp. 18-24.
29. Y. Hubenova, D. Georgiev, **M. Mitov**. Carbohydrate bioelectrosynthesis and phytate bioremediation by biofuel cells. In: Proceedings of the 6th European Fuel Cell Piero Lunghi Conference, 2015, Naples, Italy, EFC15281, pp. 317-318.
30. **M. Mitov**, I. Bardarov, Y. Hubenova. Possible applications of freshwater sediment microbial fuel cells. In: Proceedings of the 6th European Fuel Cell Piero Lunghi Conference, 2015, Naples, Italy, EFC15280, pp. 335-336.
31. E. Chorbadzhiyska, **M. Mitov**, Y. Hubenova, L. Nalbandian. NiW and NiMo Electrodeposits as cathode materials for microbial electrolysis cell. In: Proceedings of the Fifth International Scientific Conference FMNS-2013, vol. 4: Chemistry, pp. 88-96.
32. G. Hristov, E. Chorbadzhiyska, A. Evdou, L. Nalbandian, N. Dimcheva, Y. Hubenova, **M. Mitov**. Ab initio study of Pd-Au electrodeposits as anodic catalyst for Direct Borohydride Electrooxidation. In: Proceedings of the Fifth International Scientific Conference FMNS-2013, vol. 4: Chemistry, pp. 97-102.
33. G. Hristov, E. Chorbadzhiyska, R. Rashkov, Y. Hubenova, **M. Mitov**. Comparative investigation of CoMnB, CoNiMnB and CoNiMoW-supported anodes for Direct Borohydride Fuel Cells. In: Proceedings of the Fourth International Scientific Conference FMNS-2011, vol.1, Blagoevgrad, pp. 428-433.
34. G. Hristov, E. Chorbadzhiyska, R. Rashkov, Y. Hubenova, **M. Mitov**. Comparison of sodium borohydride hydrolysis kinetics on Co-based nanocomposite catalysts. In: Proceedings of the Fourth

International Scientific Conference FMNS-2011, vol.1, Blagoevgrad, pp. 295-300.

35. M. Mitov, Y. Hubenova, S. Manev. Demonstration fuel cell in chemical education. In: Proceedings of the Third International Scientific Conference FMNS-2009, vol.1, Blagoevgrad, pp.247-250.

36. M. Mitov, R. Rashkov, St. Hristov, A. Kaisheva. A novel approach to the fuel cell technology. In: Proceedings of the Third International Scientific Conference FMNS-2009, vol.2, Blagoevgrad, pp.3-10.

37. S. Babanova, Y. Hubenova, M. Mitov. Biofuel cells – alternative power sources. In: Proceedings of the Third International Scientific Conference FMNS-2009, vol.2, Blagoevgrad, pp.24-29.

38. G. Hristov, E. Hristova, M. Mitov. Investigation of metal hydride electrodes for application in Direct Borohydride Fuel Cells. In: Proceedings of the Third International Scientific Conference FMNS-2009, vol.2, Blagoevgrad, pp.167-173.

39. M. Mitov, K.Lekova (2008) UV-Spectroscopy determination of sulfide ions in alkaline solutions. *Ann. Shumen Univ.* XVIII B2: 116-121.

40. M. Mitov, R. Rashkov, N. Atanassov, A. Zielonka. Cobalt-based nanocomposites as catalysts for hydrogen generation. In: *Nanoscience & Nanotechnology*, **6**, Ed. by E. Balabanova and I. Dragieva, Heron Press, Sofia, 2006, pp.165-168.

41. M. Mitov, E. Hristova, G. Hristov, Y. Petrov, S. Hristov. Investigation of sodium borohydride conversion on nanocomposite CoMnB electrodeposits. In: Proceedings of the International Workshop “Nanostructured Materials in Electroplating”, Ed. by D. Stoychev, E. Valova, I. Krastev and N. Atanassov, St. Kliment Ohridski University Press, Sofia, 2006, pp. 213-217.

42. M. Mitov, R. Rashkov, N. Atanassov, Y. Petrov, S. Hristov, A. Kaisheva. Metal hydride – air fuel cell using alkaline borohydrides as a fuel. In: Proceedings of the Workshop “Hydrogen Technologies, Fuel Cells and Applications 2006 (HT-FCA 2006)”, Ed. by B. Horak, ISBN 80-248-1179-0, VSB-TU Ostrava, pp.7-14.